Chemical Physics 121 (1988) 63–71
North-Holland, Amsterdam

FORMATION OF NH($c\,^1\Pi$) AND NH($A^3\Pi$) IN THE PHOTOLYSIS OF NH_3, HN_3 AND HNCO AT 121.6 nm

T. HIKIDA, Y. MARUYAMA, Y. SAITO and Y. MORI

Department of Chemistry, Tokyo Institute of Technology, Meguro-ku, Ohokayama, Tokyo, Japan

Received 4 September 1987

Time profiles of the NH($c\,^1\Pi$) and NH($A^3\Pi$) fluorescence intensities were measured in the photolyses of NH_3, HN_3, and HNCO using the Lyman-α line at 121.6 nm. Upon irradiation of NH_3, only NH($c\,^1\Pi$) was observed as a primary product. The emissions from NH($c\,^1\Pi$) and NH($A^3\Pi$) were observed when HN_3 was irradiated. The NH triplet state was found to be formed by the sensitized reactions of $N_2(B\,^3\Pi_g$ and $B'\,^3\Sigma_u^-)$ with HN_3, where $N_2(B\,^3\Pi_g$, and $B'\,^3\Sigma_u^-)$ were formed as primary products in the photolysis. The dissociation processes of NH_3 and HN_3 seem to conserve their spin state. On the contrary, the time profiles of fluorescence intensity suggested that NH($c\,^1\Pi$) and NH($A^3\Pi$) were formed in the photodissociation of HNCO within the experimental time resolution of a few nanoseconds.

1. Introduction

When a photoexcited molecule dissociates, the internal states of the fragments will be determined by the incident photon energy and the dissociation pathways. Various correlation rules have been developed to suggest possible reactions to be considered. The spin correlation rule proposed by Wigner [1] is one of the useful rules, since the multiplicity of an excited molecule is often observable. This rule may be valid for the photodissociation of small molecules, but exceptions to the rule have also been reported [2].

The VUV photodecomposition of NH_3, HN_3, and HNCO to observe excited states of NH has been studied frequently. All three compounds studied are known to induce fluorescence from NH photofragments [3]. Both NH($c\,^1\Pi$) and NH($A^3\Pi$) fluoresce in the convenient spectral region of 320–340 nm. But only a few systems were investigated with a time resolved method. In this paper we report the photolysis of these molecules using the Lyman-α line at 121.6 nm in conjunction with flash fluorescence spectroscopy, which should give us important information on the photodissociation of NH_3, HN_3, and HNCO by single photon processes.

Various electronic states of NH and NH_2 photofragments have been observed but NH($A^3\Pi$) is absent in the photolysis of NH_3 by VUV light [4]. NH($A^3\Pi$) has been observed only in the presence of foreign gases such as Xe or Kr, as the results of the intersystem crossing NH($c\,^1\Pi \rightarrow A^3\Pi$) induced-by-collisions [5,6]. The direct formation of NH($A^3\Pi$) (+2H) is energetically not possible in the 121.6 nm photolysis. The laser flash photolysis of NH_3 at 193 nm [7] has been observed to form NH($A^3\Pi$) as the result of a two-photon excitation process.

The VUV photolysis of HN_3 below 160 nm has been reported to induce fluorescence originating from NH($A^3\Pi$) as well as from NH($c\,^1\Pi$). The direct formation of NH($A^3\Pi$) + $N_2(X\,^1\Sigma_g^+)$ is energetically possible but is spin-forbidden. Welge [8] has suggested that NH($A^3\Pi$) is formed by secondary reactions involving $N_2(A\,^3\Sigma_u^-)$ when HN_3 was irradiated by the Kr or Xe resonance line. Later, Okabe [9] has reinvestigated the reaction mechanism, and concluded that NH($A^3\Pi$) may be formed largely by the reaction between HN_3 and electronically excited triplet N_2, probably $N_2(B\,^3\Pi_g)$, to form NH($A^3\Pi$) + $2N_2$. Recently, preliminary measurements on time profiles of the NH($A^3\Pi$) emission intensity have been

0301-0104/88/$03.50
(North-Holland Physics Publishing Division)

reported, suggesting the formation of $N_2(B'\,^3\Sigma_u^-)$ as well as $N_2(B\,^3\Pi_g)$ in the photolysis of HN_3 at 121.6 nm [10].

Emission bands originating from NH($A\,^3\Pi$ and $c\,^1\Pi$) were observed in the photolysis of HNCO by the Kr lines accompanying with the NCO($A\,^2\Sigma^+$ and $B\,^2\Pi$) fluorescence [11]. NH($A^3\Pi$) is considered to be produced mostly by a secondary process involving CO($a\,^3\Pi$) formed in the photodecomposition of HNCO, CO($a\,^3\Pi$) + NH($X\,^3\Pi$). This mechanism is similar to that of HN_3 and the spin correlation rule is maintained, but the presence of CO($a\,^3\Pi$) has not been observed. Time profiles of NH($A^3\Pi$) emission are expected to show the presence of the metastable state, if any.

2. Experimental

Fluorescence spectra and fluorescence decay curves were measured by the technique of single photon counting in conjunction with a repetitive pulsed light source [12]. The repetition rate of the light pulser operated at 8–10 kV was usually adjusted to 4–8 kHz. The spectral feature of the output light pulses varied with the gas conditions in the discharge tube. In pure H_2 at low pressures, the output spectrum in the VUV region mostly consists of the Lyman-α line at 121.6 nm and H_2 molecular bands extending from 155 to 165 nm. The H_2 molecular bands were eliminated by an O_2 optical filter (1 atm, 1 cm). The pulse duration was observed to be about 10 ns. The present experiment is in the submicrosecond time scale, and no further attempt was made to measure accurate pulse durations.

The reaction cell was a Wood's horn type made of Pyrex glass and connected to the light source through two magnesium fluoride windows. O_2 as the light filter was introduced between the two magnesium fluoride windows [13]. The emission was observed through a fused silica window at right angles to the incident excitation light beam by a combination of a monochromator (JASCO CT-50) and a photomultiplier (HTV R585 or R649).

Fluorescence spectra were obtained by simply measuring the photon pulse rate, or for some experiments, by measuring the gated output pulse rate using a single channel analyzer connected to the TAC. This method reduced undesirable signals such as scattered light from the light source as well as "dark" counts. The pulse rate was measured by a rate meter or a multichannel scalar.

HN_3 was prepared by heating a mixture of NaN_3 and stearic acid under vacuum [9]. The outcoming gas was passed through a column of P_2O_5 powder on glass wool and then it was frozen at liquid N_2 temperature to pump non-condensable impurities. The prepared HN_3 gas was stored in a dark bottle at a pressure less than 50 Torr to avoid explosion.

HNCO was prepared by heating a mixture of NaNCO and stearic acid under vacuum [14]. Generated HNCO vapor was passed through P_2O_5 and Ag_2O columns to remove water and HCN, respectively. Then, HNCO was purified by trap-to-trap distillation in vacuo at −115 °C (ethyl alcohol). HNCO was kept at liquid nitrogen temperature to avoid polymerization. A mass spectrometric analysis showed 2–3% CO_2 impurity. Since the absorption coefficient of CO_2 is very small at 121.6 nm [11], no further purification of HNCO was performed.

Research grade NH_3, Ar, N_2, O_2 and H_2 were obtained commercially, and were used without further purification. Sample gas pressures were measured by a capacitance manometer (MKS-221). All measurements were carried out at room temperature.

3. Results and discussion

3.1. Emission spectra of NH photofragments

Figs. 1a, 1b and 1c show fluorescence spectra observed in the spectral range of 320–345 nm when NH_3 (0.1 Torr), HN_3 (0.1 Torr) and HNCO (0.08 Torr) were photolyzed at 121.6 nm, respectively. Because of the stronger emission intensity the spectral resolution is higher (0.7 nm) for the photolysis of HNCO than for the other two cases (2.0 nm).

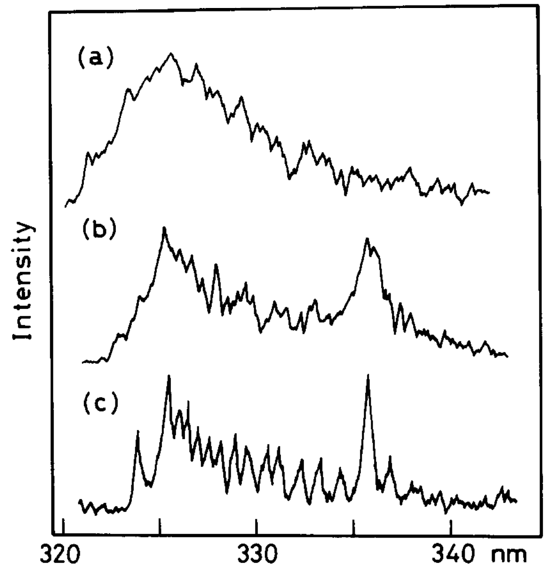

Fig. 1. Fluorescence spectra observed when (a) NH_3, (b) HN_3 and (c) HNCO were photolyzed at 121.6 nm. The sample pressures were 0.1, 0.1 and 0.08 Torr, respectively. The spectral resolutions were 2 nm for (a) and (b), and 0.7 nm for (c).

In the photolysis of NH_3 by the 121.6 nm line, the photofragments which may fluoresce are NH and NH_2 radicals in various electronic states. Fig. 1a shows the emission, NH(c $^1\Pi \rightarrow$ a $^1\Delta$) which is the only transition observed in the wavelength region of 320–345 nm. At low NH_3 pressures. NH(c $^1\Pi$) seems to be rotationally excited. An addition of Ar up to 20 Torr caused only the rotational relaxation and the singlet emission intensity remained approximately constant. The fluorescence from NH(A$^3\Pi$) was not observed as has been already reported [5] that NH(A$^3\Pi$) is not formed in the photolysis of NH_3 by H, Kr and Xe resonance lines.

Fig. 1b shows the fluorescence spectrum obtained in the photolysis of 0.1 Torr HN_3 at 121.6 nm. The transitions NH(c $^1\Pi \rightarrow$ a $^1\Delta$) and NH(A $^3\Pi \rightarrow$ X $^3\Sigma^-$) were observed with their maxima at 326 and 336 nm, respectively. In the pure HN_3 systems at low pressure, NH(c $^1\Pi$) seems to be rotationally excited and the emission extends to longer wavelengths than 336 nm where the NH(A$^3\Pi$) fluorescence superimposes. The spectrum agrees with the fluorescence spectra reported in the photolysis of HN_3 by Xe and Kr lines [9].

The HNCO photodecomposition at 121.6 nm induced fluorescence from photofragments NH(c$^1\Pi$ and A$^3\Pi$) and NCO(A$^2\Sigma^+$ and B $^2\Pi$). Fig. 1c shows the emission spectra in the wavelength region from 320 to 345 nm when 0.08 Torr HNCO was photolyzed. Similar to the cases of NH_3 and HN_3 photolyses, NH(c$^1\Pi$) is rotationally excited.

3.2. *Time profiles of the NH(c $^1\Pi$) emission*

Time profiles of fluorescence intensities were measured at 326 and 336 nm for low ($N' = 1$–5) and high ($N' \approx 14$) rotational levels of NH(c $^1\Pi$), respectively, with NH_3 pressures between 0.05

Table 1
Zero-pressure lifetimes and quenching rate constants of NH(c $^1\Pi$)

Parent molecule	Wavelength (nm)	τ_0 (ns)	k_q (10^{-10} cm^3 molecule^{-1} s^{-1})		
			parent molecule	Ar	N_2
NH_3	326 ($N' = 1$–5)	480±40	5.7±0.2	< 0.03	–
	336 ($N' \approx 14$)	310±30	5.8±0.2	0.10±0.03	–
HN_3	326 ($N' = 1$–5)	440±40	9.8±0.4	< 0.02	0.14±0.01
HNCO	326 ($N' = 2$–4)	470±50	7.2±0.3	–	–

and 0.43 Torr. Observed decay curves showed that NH($c\,^1\Pi$) was formed by the direct photodecomposition of NH_3 within the excitation light pulse width, ≈ 10 ns, and disappeared in accordance with first-order decay laws. Stern–Volmer plots of the decay rates observed at 326 and 336 nm against the pressure of NH_3 have been obtained to give good linear relation. As given in table 1, the zero-pressure lifetime at 326 nm is 480 ns, and at 336 nm is 310 ns.

The lifetime of 480 ns for lower rotational levels of NH($c\,^1\Pi$) is in an excellent agreement with reported values [15,16] and somewhat longer than those reported for individual rotational levels [17]. Shorter lifetimes for higher rotational levels are reported as an evidence of the predissociation. Our observation of 310 ns for the $N' \approx 14$ rotational level is in good agreement with a reported value [17].

The slopes of the linear plots which represent the quenching rate constants of NH($c\,^1\Pi$) by NH_3 are nearly equal for low and high rotational levels, as listed in table 1. These values are in reasonable agreement with the value reported in a steady-state experiment [5]. The quenching rates seem to be unchanged for rotational levels of $N' \leqslant 14$ [18]. Decay rates were also measured in the presence of Ar. The quenching rate constant observed at 336 nm is much larger than that observed at 326 nm suggesting the presence of rotational relaxation in NH($c\,^1\Pi$) by Ar. In fact, the time profile of the NH($c\,^1\Pi$) fluorescence observed at 326 nm in the presence of Ar indicated the rotational relaxation by a slight, slow rise of the fluorescence intensity superimposed on the single exponential decay of the NH($c\,^1\Pi$) fluorescence.

The time profiles of NH($c\,^1\Pi$) fluorescence intensities were measured at 326 nm in the photolyses of HN_3 and HNCO. In both cases, NH($c\,^1\Pi$) is evidently formed by photodecomposition within the excitation light pulse width of ≈ 10 ns, and decay in accordance with first-order decay laws. Stern–Volmer plots of the decay rates versus the pressures of HN_3 and HNCO gave linear relations. From the slopes and intercepts, the quenching rate constants and the zero-pressure lifetime of NH($c\,^1\Pi$) are obtained. The quenching rate constant, 9.8×10^{-10} cm^3 molecule^{-1} s^{-1} for HN_3 is close to that of ref. [15] and slightly larger than the reported value of ref. [16]. The zero-pressure lifetime is obtained to be 440 or 470 ns. Together with the lifetime obtained in the NH_3 photolysis, the averaged lifetime of NH($c\,^1\Pi$), 460 ± 60 ns is in good agreement with previous studies [5,15–17]. From similar experiments, quenching rate constants for Ar and N_2 were obtained. These are also listed in table 1.

3.3. *Time profiles of NH($A\,^3\Pi$) emission*

3.3.1. *Photolysis of NH_3*

Emission from NH($A\,^3\Pi$) was not observed at NH_3 pressures lower than 0.5 Torr. In the presence of O_2 the fluorescence from NH($c\,^1\Pi$) was strongly quenched, and the NH($A\,^3\Pi$) fluorescence appeared instead. Time profiles of the triplet fluorescence intensity at 336 nm were given by a function containing two exponential terms, a rise and a decay component, which correspond to the decay rates of NH($c\,^1\Pi$) and NH($A\,^3\Pi$), respectively. For the O_2 pressure up to 1.0 Torr, the measured decay rates are in agreement with those of NH($c\,^1\Pi$) and NH($A\,^3\Pi$). The results are consistent with the collision-induced formation mechanism of NH($A\,^3\Pi$) [5,6], which seems to be well established now.

3.3.2. *Photolysis of HN_3*

In the photolysis of HN_3 by the 121.6 nm line, time profiles of the NH fluorescence at 336 nm were observed to be complex. It is expected that the NH($c\,^1\Pi$) fluorescence superimposes as already mentioned. In fig. 2 the dots show the time profile observed at 336 nm when 0.06 Torr HN_3 was photolyzed at 121.6 nm. It consists of three decay components. The slower components seem to exhibit initial gradual increases in intensities though they are not readily seen due to the superimposed fast component. The fast component is probably that of NH($c\,^1\Pi$, $N' \approx 14$) and is strongly affected by the presence of Ar or N_2. Slower decays in the time domain of several microseconds cannot be attributed to electronically excited states of NH.

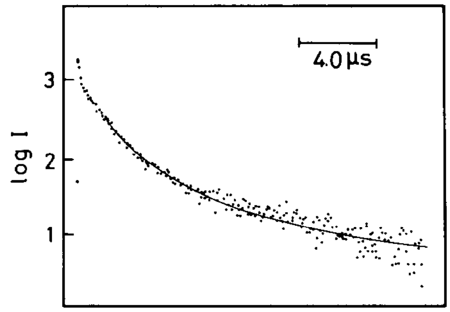

Fig. 2. Time profile of NH($A^3\Pi$) fluorescence when 0.06 Torr HN_3 was photolyzed at 121.6 nm. The solid line is the best fitted convoluted curve assuming a double exponential decay function with 1.3 and 6.9 μs lifetimes.

In order to estimate the lifetimes of the two slow components, the later parts of decay curves were analyzed assuming double exponential decay functions. The best fitted convoluted curve to the data is shown in fig. 2 by the solid line, which contains 1.3 and 6.9 μs lifetimes. A similar analysis was carried out for experimental results with various HN_3 pressures. The resulting Stern–Volmer plots of the two decay components are shown in fig. 3. From the intercepts and the slopes, the zero-pressure lifetimes and the quenching rate constants for HN_3 were obtained to be 2.7 μs and 2.6×10^{-10} cm^3 molecule^{-1} s^{-1} for the fast component, and for the slow one the obtained values are 18 μs and 4.9×10^{-11} cm^3 molecule^{-1} s^{-1}, respectively.

The lifetimes, 2.7 and 18 μs, are much longer than that of NH($A^3\Pi$) which is reported to be 500 ns and seem to reflect the lifetimes of other energetic photofragments. NH($A^3\Pi$) may be formed by secondary reactions between energetic intermediates and HN_3. In this system, candidates for the microsecond lifetimes are triplet N_2 molecules which may be formed in the photolysis of HN_3.

When NH($A^3\Pi$) is formed by secondary reactions involving triplet N_2, the time profile of the NH($A^3\Pi$) fluorescence must have an initial delayed increase in intensity corresponding to the NH($A^3\Pi$) lifetime under a given experimental condition ($\leqslant$ 500 ns) followed by slow decay characteristics of N_2 triplet states. In order to observe the rises more clearly, time profiles were measured at 336 nm in the presence of Ar, which quenches the rotational energy of $c^1\Pi$ and isolates the $A^3\Pi$ emission bands from those of $c^1\Pi$. Fig. 4 (dots) shows an intensity time profile of the NH fluorescence observed at 336 nm when 0.1 Torr HN_3 was photolyzed by the 121.6 nm light pulse in the presence of Ar at 8.0 Torr. It clearly shows an initial delayed increase in intensity.

For analysis of the fluorescence time profiles having three different lifetimes, the following

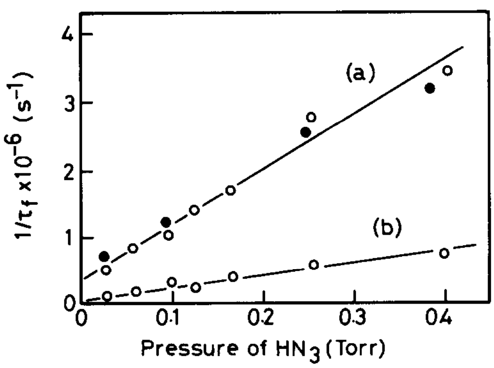

Fig. 3. Stern–Volmer plots of (a) fast and (b) slow decay rates against the pressure of HN_3. In (a) decay rates observed at 660 nm, the N_2 first positive band are indicated by ●.

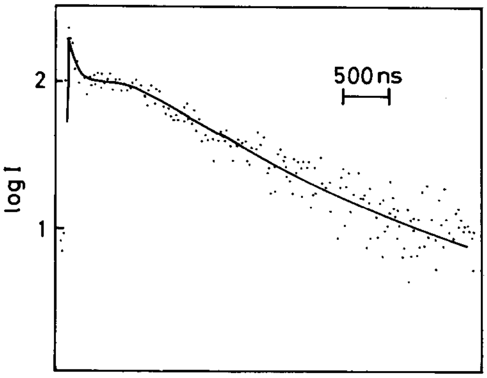

Fig. 4. Time profile of the NH fluorescence observed at 336 nm when 0.1 Torr HN_3 was photolyzed by the 121.6 nm light pulse in the presence of Ar at 8.0 Torr.

mechanism was assumed under low pressure conditions:

$$\mathrm{HN_3} + h\nu \rightarrow \mathrm{NH(c\,^1\Pi)} + \mathrm{N_2(X\,^1\Sigma_g^+)}, \tag{1a}$$

$$\rightarrow \mathrm{N_2^*(T)} + \mathrm{NH(X\,^3\Sigma^-)}, \tag{1b}$$

$$\rightarrow \mathrm{N_2^{**}(T)} + \mathrm{NH(X\,^3\Sigma^-)}, \tag{1c}$$

$$\rightarrow \text{others}. \tag{1d}$$

$$\mathrm{NH(c\,^1\Pi)} \rightarrow \mathrm{NH(a\,^1\Delta)} + h\nu_1, \tag{2}$$

$$\mathrm{N_2^*(T)} + \mathrm{HN_3} \rightarrow \mathrm{NH(A\,^3\Pi)} + 2\mathrm{N_2(X\,^1\Sigma_g^+)}, \tag{3}$$

$$\mathrm{N_2^{**}(T)} + \mathrm{HN_3} \rightarrow \mathrm{NH(A\,^3\Pi)} + 2\mathrm{N_2(X\,^1\Sigma_g^+)}, \tag{4}$$

$$\mathrm{NH(A\,^3\Pi)} \rightarrow \mathrm{NH(X\,^3\Sigma^-)} + h\nu_2, \tag{5}$$

$$\mathrm{N_2^*(T)} \rightarrow \mathrm{N_2(X\,^1\Sigma_g^+)} + h\nu_3, \tag{6}$$

$$\mathrm{N_2^{**}(T)} \rightarrow \mathrm{N_2(X\,^1\Sigma_g^+)} + h\nu_4, \tag{7}$$

where $N_2^*(T)$ and $N_2^{**}(T)$ denote N_2 triplet states which sensitize the NH($A^3\Pi$) fluorescence.

Reaction (1a) is responsible for the formation of the singlet state and reactions (1b) and (1c) are for the triplet formation. NH($c^1\Pi$) gives fluorescence emission at 326 nm via reaction (2). Both triplet N_2 are supposed to sensitize HN_3 to form NH($A^3\Pi$) via reactions (3) and (4), and eventually gives the NH($A^3\Pi$) fluorescence at 336 nm, reaction (5). Decay rates of the fluorescence intensity are determined largely by reactions (3) and (4). Reactions (6) and (7) represent the emissive decay channels of the metastable N_2 triplet states, presumably in the visible and infrared regions.

If reaction (1) is very fast and occurs within the duration of photolysis light pulses the intensity of NH($c^1\Pi$) fluorescence is described as,

$$I_a(t) = A\exp(-k_2 t), \tag{8}$$

where A is constant, and k_2 is the decay rate of NH($c^1\Pi$). The intensity of NH($A^3\Pi$) emission is described as the sum of the equations

$$I_b(t) = B[-\exp(-k_5 t) + \exp(-k_3' t)], \tag{9}$$

$$I_c(t) = B'[-\exp(-k_5 t) + \exp(-k_4' t)], \tag{10}$$

where B and B' are constants, k_5 is the decay rate of NH($A^3\Pi$), and k_3' and k_4' are the decay rates of $N_2^*(T)$ and $N_2^{**}(T)$, respectively. Under higher-pressure conditions, quenchings of excited species may take place, and therefore, eqs. (8)–(10) represent functions of the pressure. The observed intensity time profiles, $I(t)$, were simulated as

$$I(t) = I_a(t) + I_b(t) + I_c(t). \tag{11}$$

The best fitted simulated curve is shown in fig. 4 by a solid line. The three different components are: $I_a(t)$, < 10 ns fast rise followed by a single exponential decay with a lifetime of $1/k_2 = 75$ ns, $I_b(t)$, slower rise ($1/k_5 = 340$ ns) followed by a $1/k_3 = 940$ ns decay, and $I_c(t)$, slower rise ($1/k_5 = 340$ ns) and very slow decay ($1/k_4' = 3.5$ μs). The relative values estimated for A, B and B' are 1 : 0.8 : 0.3. The obtained k_3, k_4, and k_5 are found to be independent of the Ar pressure between 5 and 20 Torr, but dependent on the pressure of HN_3.

The rate constant of the slow rise component k_5 in $I_b(t)$ and $I_c(t)$ was measured at various HN_3 pressures. Stern–Volmer plots for k_5 versus HN_3 pressure are shown in fig. 5. The plots fit a straight line with a zero-pressure lifetime of 500 ns. The quenching rate constant by HN_3, $4.7 \times 10^{-10}\ \mathrm{cm^3\ molecule^{-1}\ s^{-1}}$ was obtained from the slope. The observed lifetime is in agreement with that of NH($A^3\Pi$). This indicates that the same NH($A^3\Pi$) is formed by secondary reactions of two different intermediate species. The absence of a fast rise of the NH($A^3\Pi$) fluorescence suggests

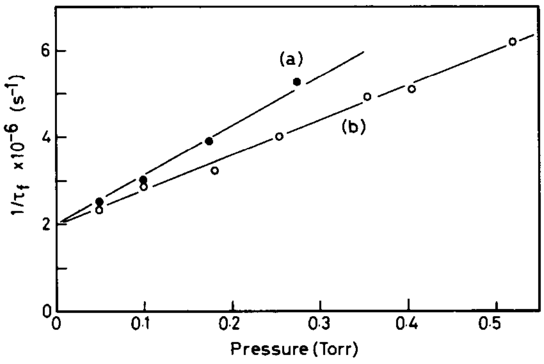

Fig. 5. Stern–Volmer plots of the NH($A^3\Pi$) fluorescence decay. (a) Best fitted decay rates (k_5) obtained by eq. (11) versus the pressure of HN_3. (b) NH($A^3\Pi$) decay rate versus HNCO.

that the direct formation of NH($A^3\Pi$) seems to be a minor process.

NH($A^3\Pi$) is mainly produced in the secondary reactions between HN_3 and excited triplet N_2 molecules initially formed in the 121.6 nm photolysis of HN_3. Energetically available N_2 triplet states are $A^3\Sigma_u^+$, $B\,^3\Pi_g$, $B'\,^3\Sigma_u^-$, and $W\,^3\Delta_u$ [19]. $N_2(A^3\Sigma_u^+)$, and $N_2(W\,^3\Delta_u)$ have too long lifetimes, 2.0 s [20] and 0.49 ms ($v = 2$) [21], respectively. Lifetimes of various vibrational levels of $N_2(B\,^3\Pi_g)$ have been reported frequently. Reported lifetimes are in agreement within a factor of 2, ranging from 2.2 to 8.0 μs depending on vibrational levels [22–28]. As a general trend, shorter lifetimes have been observed for higher vibrational levels. The lifetime of $N_2(B'\,^3\Sigma_u^-)$ has not yet been measured, but the radiative lifetime is expected to be similar to that of $N_2(B\,^3\Pi_g)$ since both states undergo the same type of electronic transition. $\pi_u 2P \to \sigma_g 2P$ for $N_2(B\,^3\Pi_g \to A^3\Sigma_u^+)$ and $\sigma_g 2P \to \pi_u 2P$ for $N_2(B'\,^3\Sigma_u^- \to B\,^3\Pi_g)$. An estimated value for $N_2(B'\,^3\Sigma_u^-)$ has been reported to be 24–27 μs [29]. The shorter component with a lifetime of 2.7 μs may be attributed to $N_2(B\,^3\Pi_g)$ and the longer one with its lifetime of 18 μs to $N_2(B'\,^3\Sigma_u^-)$.

Emission from $N_2(B\,^3\Pi_g)$ appears in the wavelength region from 600 to 1100 nm [29,30]. Intensity time profiles at 660 nm where the N_2 first positive system ($B\,^3\Pi_g$, $v' = 4 \to A^3\Sigma_u^+$, $v'' = 1$) appears, were measured in the photolysis of HN_3 at 121.6 nm using an interference band-pass filter (Shonan kogaku No. 8307-446, 660 ± 5 nm). The decay rates thus obtained are plotted in fig. 3 by closed circles: it clearly shows that the zero-pressure lifetime of 2.7 μs may be attributed to $N_2(B\,^3\Pi_g)$. Zero-pressure lifetimes and quenching rate constants for $N_2(B\,^3\Pi_g)$, $N_2(B'\,^3\Sigma_u^-)$, and NH($A^3\Pi$) obtained from analysis of the intensity time profiles at 336 and at 660 nm are summarized in table 2.

In the photolysis of HN_3 at 121.6 nm, three different dissociation channels were observed with respect to the excited NH formation. The reaction scheme previously given may be rewritten as follows:

$$HN_3 + h\nu \to NH(c\,^1\Pi) + N_2(X\,^1\Sigma_g^+), \qquad (1a')$$

$$\to NH(X\,^3\Sigma^-) + N_2(B\,^3\Pi_g), \qquad (1b')$$

$$\to NH(X\,^3\Sigma^-) + N_2(B'\,^3\Sigma_u^-). \qquad (1c')$$

The formation of NH($A^3\Pi$) can be expressed by the following secondary reactions involving $N_2(B\,^3\Pi_g)$ and $N_2(B'\,^3\Sigma_u^-)$,

$$N_2(B\,^3\Pi_g) + HN_3 \to NH(A^3\Pi) + 2N_2(X\,^1\Sigma_g^+), \qquad (3')$$

$$N_2(B'\,^3\Sigma_u^-) + HN_3 \to NH(A^3\Pi) + 2N_2(X\,^1\Sigma_g^+). \qquad (4')$$

The intensity ratio of the NH($A^3\Pi$) and NH($c\,^1\Pi$) emission increased with the pressure of HN_3. At 0.01 Torr of HN_3 pressure the NH($A^3\Pi$) emission was vanishingly weak compared to that from NH($c\,^1\Pi$).

3.3.3. Photolysis of HNCO

Fig. 6 shows a typical time profile of the fluorescence intensity of NH($A^3\Pi$) observed at 336 nm in the photolysis of HNCO at 121.6 nm. Though the rotationally excited NH($c\,^1\Pi$) fluorescence extends to longer wavelengths than 336 nm,

Table 2
Zero-pressure lifetimes and quenching rate constants of HN($A\,^3\Pi$) $N_2(B\,^3\Pi_g)$ and $N_2(B'\,^3\Sigma_u^-)$

	Wavelength (nm)	τ_0	k_q (10^{-10} cm^3 molecule^{-1} s^{-1})	
			HN_3	HNCO
NH($A\,^3\Pi$)	336	500 ± 40 ns	4.7 ± 0.1	4.3 ± 0.3
$N_2(B\,^3\Pi_g)$	336, 660	2.7 ± 0.2 μs	2.6 ± 0.2	–
$N_2(B'\,^3\Sigma_u^-)$	326	18 ± 2 μs	0.46 ± 0.03	–

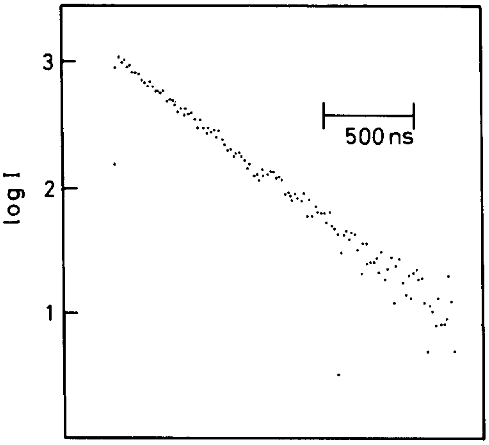

Fig. 6. Typical time profile of the fluorescence intensity of NH($A^3\Pi$) in the photolysis of 0.07 Torr HNCO at 121.6 nm.

the spectral resolution of 0.7 nm was high enough to isolate the NH($A^3\Pi$) emission band from the $c^1\Pi$ emission band. The initial very fast rise of the fluorescence intensity closely corresponds to the duration of the excitation light pulse (≈ 10 ns). It is not possible to identify the slow rise of the fluorescence intensity which corresponds to the indirect formation of NH($A^3\Pi$) via reactions with some long-lived precursors. The fluorescence decay profiles obtained in this experiment were well represented by a single exponential decay function.

In fig. 5b Stern–Volmer plots of decay rates for various HNCO pressures are shown. The self-quenching rate constant and the zero-pressure lifetime were calculated from the slope and the intercept, and are summarized in table 2. The lifetime of 500 ns is in good agreement with the one obtained in the previous section and the reported lifetime of NH($A^3\Pi$) [15–17].

Based on the spin conservation rule, it has been suggested [11] that NH($A^3\Pi$) should be produced mostly by a secondary process involving CO($a\,^3\Pi$), which is considered to be a direct photodissociation product of the excited HNCO. No evidence, however, was observed to indicate the presence of CO($a\,^3\Pi$) in time resolved measurements of NH($A^3\Pi$) fluorescence. If CO($a\,^3\Pi$) is involved in the formation of NH($A^3\Pi$), its fluorescence intensity should increase slowly as the CO($a\,^3\Pi$) concentration decreases. Under the present experimental conditions. CO($a\,^3\Pi$) may last much longer than 100 ns [31].

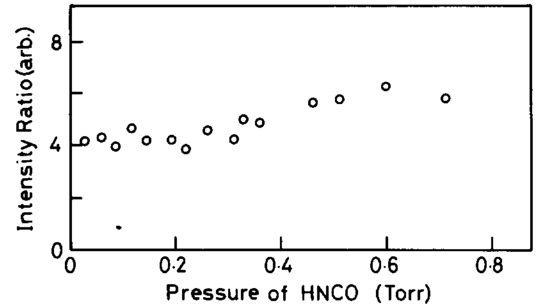

Fig. 7. Intensity ratio of the singlet and the triplet fluorescence against the pressure and HNCO. Differences in the quenching rate are corrected.

The intensity of NH($A^3\Pi$) fluorescence relative to that of NH($c^1\Pi$) was approximately constant for the pressure of HNCO between 0.05 and 0.7 Torr as shown in fig. 7. Differences in quenching rates by HNCO were corrected accordingly. Emission from NH($c^1\Pi$) is about 5 times more intense than that from NH($A^3\Pi$). These data suggest that NH($A^3\Pi$) is formed directly in the photolysis of HNCO. The slight tendency to increase the ratio at higher pressures may indicate the presence of the secondary process.

Though the process is only a minor one, the "spin-forbidden" dissociation reaction is observed only in the photolysis of HNCO at 121.6 nm. Both the singlet and the triplet HNCO may be formed before the dissociation takes place. At the moment, it is not clear why the nature of the excited HNCO is much different from the others. The HNCO excited at 121.6 nm may have a longer lifetime than that of NH_3 or HN_3, which allows a part of the excited molecules to cross to the triplet state.

Acknowledgement

The authors are grateful to Professor Tsunashima and Dr. Umemoto for giving us much information prior to publication. This work was partially supported by a Grant-in-Aid for Science Research No. 62606508 from the Ministry of Education, Science, and Culture.

References

[1] E. Wigner and E.E. Witmer, Z. Physik 51 (1928) 859.
[2] H. Okabe, J. Chem. Phys. 56 (1972) 4381.
[3] H. Okabe, Photochemistry of small molecules (Wiley, New York, 1978).
[4] K.H. Becker and K.H. Welge, Z. Naturforsch 18a (1963) 600.
[5] M. Kawasaki, Y. Hirata and I. Tanaka, J. Chem. Phys. 59 (1973) 648.
[6] F. Rohrer and F. Stuhl, J. Chem. Phys. 86 (1987) 226.
[7] H.K. Haak and F. Stuhl, J. Phys. Chem. 88 (1984) 2201.
[8] K.H. Welge, J. Chem. Phys. 45 (1966) 4673.
[9] H. Okabe, J. Chem. Phys. 49 (1968) 2726.
[10] Y. Maruyama, T. Hikida and Y. Mori, Chem. Phys. Letters 116 (1985) 371.
[11] H. Okabe, J. Chem. Phys. 53 (1970) 3507.
[12] Y. Saito, T. Hikida, T. Ichimura and Y. Mori, J. Chem. Phys. 80 (1984) 31.
[13] T. Hikida, J.A. Eyre and L.M. Dorfman, J. Chem. Phys. 54 (1971) 3422.
[14] G.T. Fujimoto, M.E. Umstead and M.C. Lin, Chem. Phys. 65 (1982) 197.
[15] H.K. Haak and F. Stuhl, J. Phys. Chem. 88 (1984) 3627.
[16] H. Umemoto, J. Kikuma, S. Tsunashima and S. Sato, Chem. Phys. 120 (1988) 461.
[17] W.H. Smith, J. Brozozowski and P. Erman, J. Chem. Phys. 64 (1976) 4628.
[18] H. Obata and T. Hikida, unpublished results.
[19] K.P. Huber and G. Herzberg, Constants of diatomic molecules (Van Nostrand, Princeton, 1978).
[20] M. Jeunehomme and A.B.F. Duncan, J. Chem. Phys. 41 (1976) 4628.
[21] R. Covey, K.A. Saum and W. Benesch, J. Opt. Soc. Am. 63 (1973) 592.
[22] M. Jeunehomme, J. Chem. Phys. 45 (1966) 1805.
[23] H.J. Hartfuss and A. Schmillen, Z. Naturforsch. 23a (1968) 722.
[24] M. Hollstein, D.C. Lorents, J.R. Peterson and J.R. Scheridan, Can. J. Chem. 47 (1969) 1858.
[25] A.W. Johnson and R.G. Fowler, J. Chem. Phys. 53 (1970) 65.
[26] D.E. Shemansky and A.L. Broadfoot, J. Quant. Spectry. Radiative Transfer 11 (1971) 1385.
[27] S.T. Chen and R.J. Anderson, Phys. Rev. A 12 (1975) 468.
[28] E.E. Eyler and F.M. Pipkin, J. Chem. Phys. 79 (1983) 3654.
[29] E.M. Gartner and B.A. Thrush, Proc. Roy. Soc. A 346 (1975) 103.
[30] E.M. Gartner and B.A. Thrush, Proc. Roy. Soc. A 346 (1975) 121.
[31] G.W. Taylor and D.W. Setser, J. Chem. Phys. 58 (1973) 4840.